ROUTING AND ACTION

MEMORANDUM

ROUTING

TO:(1) Energy Sciences Branch (ES) (Gerhold, Michael)

Report is available for review

(2) Proposal Files Report No.: Proposal Number: 70190-ES.6

DESCRIPTION OF MATERIAL

CONTRACT OR GRANT NUMBER: W911NF-17-1-0109

INSTITUTION: University of Michigan - Ann Arbor

PRINCIPAL INVESTIGATOR: Zetian Mi

TYPE REPORT: Final Report

DATE RECEIVED: 9/5/22 12:32PM

PERIOD COVERED: 2/13/17 12:00AM through 5/12/21 12:00AM

TITLE: Final Report: Electrically Injected 280 nm AlGaN Nanowire Edge-Emitting Lasers

ACTION TAKEN BY DIVISION

(x) Report has been reviewed for technical sufficiency and IS [x] IS NOT [ ] satisfactory.

( ) Based on my technical review, I have identified no OPSEC or Technology Protection concerns that need to be addressed regarding this report.

(x) Perfomance of the research effort was accomplished in a satisfactory manner and all other technical requirements have been fulfilled.

(x) Based upon my knowledge of the research project, I agree with the patent information disclosed.

Approved by SSL\MICHAEL.D.GERHOLD on 9/6/22 5:49PM

ARO FORM 36-E

REPORT DOCUMENTATION PAGE

Form Approved OMB NO. 0704-0188

1. REPORT DATE (DD-MM-YYYY)	2. REPORT TYPE	3. DATES COVERED (From - To)
05-09-2022	Final Report	13-Feb-2017 - 12-May-2021

4. TITLE AND SUBTITLE
Final Report: Electrically Injected 280 nm AlGaN Nanowire Edge-Emitting Lasers

5a. CONTRACT NUMBER
W911NF-17-1-0109

5b. GRANT NUMBER

5c. PROGRAM ELEMENT NUMBER
611102

6. AUTHORS

5d. PROJECT NUMBER

5e. TASK NUMBER

5f. WORK UNIT NUMBER

7. PERFORMING ORGANIZATION NAMES AND ADDRESSES
University of Michigan - Ann Arbor
3003 South State Street

Ann Arbor, MI 48109 -1274

8. PERFORMING ORGANIZATION REPORT NUMBER

9. SPONSORING/MONITORING AGENCY NAME(S) AND ADDRESS (ES)
U.S. Army Research Office
P.O. Box 12211
Research Triangle Park, NC 27709-2211

10. SPONSOR/MONITOR'S ACRONYM(S)
ARO

11. SPONSOR/MONITOR'S REPORT NUMBER(S)
70190-ES.6

12. DISTRIBUTION AVAILIBILITY STATEMENT
Approved for public release; distribution is unlimited.

13. SUPPLEMENTARY NOTES
The views, opinions and/or findings contained in this report are those of the author(s) and should not contrued as an official Department of the Army position, policy or decision, unless so designated by other documentation.

14. ABSTRACT

15. SUBJECT TERMS

16. SECURITY CLASSIFICATION OF:			17. LIMITATION OF ABSTRACT	15. NUMBER OF PAGES	19a. NAME OF RESPONSIBLE PERSON
a. REPORT	b. ABSTRACT	c. THIS PAGE			Zetian Mi
UU	UU	UU	UU		19b. TELEPHONE NUMBER
					734-764-3963

RPPR Final Report
as of 06-Sep-2022

Agency Code: 21XD

Proposal Number: 70190ES **Agreement Number: W911NF-17-1-0109**
INVESTIGATOR(S):

Name: Zetian Mi
Email: ztmi@umich.edu
Phone Number: 7347643963
Principal: Y

Organization: **University of Michigan - Ann Arbor**
Address: 3003 South State Street, Ann Arbor, MI 481091274
Country: USA
DUNS Number: 073133571 EIN: 386006309

Report Date: 12-Aug-2021 Date Received: 05-Sep-2022
Final Report for Period Beginning 13-Feb-2017 and Ending 12-May-2021
Title: Electrically Injected 280 nm AlGaN Nanowire Edge-Emitting Lasers
Begin Performance Period: 13-Feb-2017 **End Performance Period:** 12-May-2021
Report Term: 0-Other

Submitted By: Zetian Mi Email: ztmi@umich.edu
Phone: (734) 764-3963

Distribution Statement:

STEM Degrees: 3 **STEM Participants:**

Major Goals: Mid and deep ultraviolet (UV) light sources, including light emitting diodes (LEDs) and laser are required for many demanding applications ranging from materials processing, surface treatment, chemical and biological analysis to water purification and disinfection. To date, however, there have been no demonstrations of electrically injected AlGaN quantum well lasers with operation wavelengths less than 330 nm. The poor performance of deep UV optoelectronic devices is directly related to the presence of large densities of dislocations (typically in the range of 108 cm-2, or higher), strong polarization field and the related quantum-confined Stark effect, and extremely poor p-type conductivity of AlN and AlGaN (hole concentration in AlN typically limited to ~ 1013 cm-3, or less).

In this context, significant progress has been made in the epitaxy and characterization of AlGaN nanowire heterostructures. Nearly dislocation-free AlGaN nanowire arrays can be grown directly on low-cost, large-area Si and sapphire substrate. We have discovered, both experimentally and theoretically, that Mg-dopant incorporation is significantly enhanced in nearly defect-free III-nitride nanowire structures compared to their bulk counterparts, thereby leading to very efficient p-type conduction in wide bandgap Al-rich AlGaN that was not previously possible. The free hole concentration in AlN nanowires is measured to be ~ 1017 cm-3, which is several orders of magnitude higher compared to that of previously reported AlN epilayers. In this project, we propose to investigate the design, epitaxy, fabrication and testing of AlGaN nanowire edge-emitting lasers. The device heterostructure consists of highly uniform AlGaN dot-in-nanowire arrays grown on sapphire or Si substrate using the technique of selective area growth by molecular beam epitaxy, which enables a precise control of the size, spacing and shape of nanowires and therefore can lead to low loss waveguides. The incorporation of self-organized quantum dots in nearly defect-free AlGaN nanowire active region will lead to large gain and differential gain, due to the near-discrete density of states related to the three-dimensional (3D) quantum-confinement of charge carriers. We propose to demonstrate high performance electrically injected semiconductor laser diodes operating at the mid and deep UV.

Accomplishments: Some of the major achievements of this project include: i) Achievement of selective area epitaxy of AlGaN nanowires across nearly the entire compositional range; ii) First demonstration of electrically pumped AlGaN nanowire photonic crystal UV laser diode, which operates at 369.5 nm at room temperature with a low threshold current density of 10.6 mA under continuous wave operation; iii) Demonstration of electrically injected plasmonic UV quantum dot laser diodes, which are the shortest wavelengths ever reported for any semiconductor plasmonic lasers. These studies provide a viable path for the achievement of low threshold mid and deep UV laser diodes.

RPPR Final Report
as of 06-Sep-2022

Please refer to the attached pdf file for detailed description of the major achievements.

Training Opportunities: This project has contributed to the training of PhD students H.W. Kim, D. Laleyan, X. Liu, K. Mashooq, A. Pandey, Y. Wu, and postdoctoral researchers Y. Sun and X. Liu.

RPPR Final Report
as of 06-Sep-2022

Results Dissemination: Journal Papers:

1) D.A. Laleyan, S. Zhao, S.Y. Woo, H.N. Tran, H.B. Le, T. Szkopek, H. Guo, G.A. Botton, and Z. Mi, “AlN/h-BN Heterostructures for Mg Dopant-Free Deep Ultraviolet Photonics,” Nano Lett., vol. 17, no. 6, pp. 3738–3743, 2017.
2) X. Liu, S. Zhao, B. H. Le, and Z. Mi, “Molecular beam epitaxial growth and characterization of AlN nanowall deep UV light emitting diodes,” Applied Physics Letters, vol. 111, 101103, 2017.
3) Y. Wu, Y. Wang, K. Sun, A. Aielloa, P. Bhattacharya, Z. Mi, “Molecular beam epitaxy and characterization of Mg-doped GaN epilayers grown on Si (0 0 1) substrate through controlled nanowire coalescence,” J. Crystal Growth, vol. 498, 109, 2018.
4) X. Liu, K. Mashooq, T. Szkopek, and Z. Mi, “Improving the Efficiency of Transverse Magnetic Polarized Emission from AlGaN Based LEDs by Using Nanowire Photonic Crystal,” IEEE Photon. J., vol. 10, 4501211, 2018.
5) Invited: X. Liu, K. Mashooq, D. A. Laleyan, E. T. Reid, and Z. Mi, “AlGaN nanocrystals: building blocks for efficient ultraviolet optoelectronics,” Photonics Research, vol. 7. No. 6, B12, 2019.
6) B. H. Le, X. Liu, N. H. Tran, S. Zhao, and Z. Mi, “An Electrically Injected AlGaN Nanowire Defect-free Photonic Crystal Ultraviolet Laser,” Opt. Exp., vol. 27, 5843, 2019.
7) X. Hai, R. T. Rashid, S. M. Sadaf, Z. Mi, and S. Zhao, “Effect of low hole mobility on the efficiency droop of AlGaN nanowire deep ultraviolet light emitting diodes,” Appl. Phys. Lett., vol. 114m 101104, 2019.
8) Invited: S. Zhao, and Z. Mi, “AlGaN Nanowires: Path to Electrically Injected Semiconductor Deep Ultraviolet Lasers,” IEEE J. Quantum Electron., vol. 54, 1, 2018.
9) Y. Wu, D. A. Laleyan, Z. Deng, C. Ahn, A. F. Aiello, A. Pandey, X. Liu, P. Wang, K. Sun, E. Ahmadi, Y. Sun, M. Kira, P. K. Bhattacharya, E. Kioupakis, and Z. Mi, Controlling Defect Formation of Nanoscale AlN: Towards Efficient Current Conduction of Ultrawide-Bandgap Semiconductors, Adv. Electron. Mater., 2000337, 2020.
10) D. A. Laleyan, N. Fernández-Delgado, E. T. Reid, P. Wang, A. Pandey, G. A. Botton, Z. Mi, Strain-free ultrathin AlN epilayers grown directly on sapphire by high-temperature molecular beam epitaxy, Applied Physics Letters 116 (15), 152102.
11) X. Liu, F. A. Chowdhury, S. Vanka, S. Chu, and Z. Mi, Emerging Applications of III-Nitride Nanocrystals, Phys. Status Solidi A 2020, 1900885, 2020.

Conference Presentations:

D.A. Laleyan, S. Zhao, S.Y. Woo, H.N. Tran, B.H. Le, T. Szkopek, H. Guo, G.A. Botton, and Z. Mi, “AlN/h-BN Nanowire Heterostructures for Deep Ultraviolet Photonics,” presented at the 12th International Conference on Nitride Semiconductors, Strasbourg, France, Jul. 2017.
B.H. Le, S. Zhao, X. Liu, S.Y. Woo, G.A. Botton, and Z. Mi, “Controlled Coalescence of AlGaN Nanowire Arrays: An Architecture for Nearly Dislocation-Free Planar Ultraviolet Photonic Device,” presented at the 12th International Conference on Nitride Semiconductors, Strasbourg, France, Jul. 2017.
X. Liu, B.H. Le, S. Zhao, and Z. Mi, “Ultraviolet AlGaN Nanowire Light Emitting Diodes Operating at 279 nm by Selective Area Epitaxial Growth,” presented at the 12th International Conference on Nitride Semiconductors, Strasbourg, France, Jul. 2017.
S. Zhao, S. Sadaf, and Z. Mi, “AlGaN Nanowire Tunnel Junction LEDs in the UV-C Band,” presented at the 12th International Conference on Nitride Semiconductors, Strasbourg, France, Jul. 2017.
X. Liu, S. Zhao, B.H. Le, and Z. Mi, “Molecular Beam Epitaxial Growth and Characterization of AlN Nanowall Deep UV Light Emitting Diodes,” presented at the 12th International Conference on Nitride Semiconductors, Strasbourg, France, Jul. 2017.
X. Liu, S. Zhao, B.H. Le, and Z. Mi, “Molecular Beam Epitaxial Growth and Characterization of AlN Nanowall Deep UV Light Emitting Diodes,” presented at the 59th Electronic Materials Conference, South Bend, Indiana, USA, Jun. 2017.
Invited: Z. Mi, “Emerging Applications of III-Nitride Nanostructures: From Deep Ultraviolet Photonics to Artificial Photosynthesis,” presented at the 17th Canadian Semiconductor Science and Technology Conference, Waterloo, Ontario, Canada, Aug. 2017.
Invited: Z. Mi, “Electrically injected AlGaN nanowire deep ultraviolet lasers on Si,” presented at the Conference on Lasers and Electro-Optics – Pacific Rim, Singapore, Jul. 2017.
Invited: Z. Mi, “AlGaN deep ultraviolet tunnel junction nanowire LEDs and electrically pumped lasers,” presented at the International Conference on Nitride Semiconductors, Strasbourg, France, Jul. 2017.
Invited: Z. Mi, “AlGaN nanowire UV-C photonics,” presented at the IEEE Photonics Society Summer Topical Meeting, San Juan, Puerto Rico, Jul. 2017.
Invited: Z. Mi, “AlGaN nanowire deep ultraviolet light emitting diodes and lasers,” presented at the Conference on Lasers and Electro-Optics Europe, Munich, Germany, Jun. 2017.
Invited: Z. Mi, “Electronic structure of III-nitride nanowires for efficient light emitters and solar fuels generation,” presented at the Nanowires and Nanowire Growth Workshop, Lund, Sweden, May 2017.

Invited: Z. Mi, “AlGaN deep ultraviolet optoelectronics,” IEEE Research and Applications of Photonics in Defense Conference, Miramar Beach, FL, Aug. 22-24, 2018.
Invited: Z. Mi, “AlGaN Nanowire Deep Ultraviolet Photonics,” 233rd ECS Meeting, Seattle, WA, May 13-17, 2018.
Keynote: Z. Mi, “AlGaN nanowire LEDs and laser diodes operating in the UV-C band,” International Workshop on UV Materials and Devices (IWUMD), Fukuoka, Japan, Nov. 14-18, 2017.
Invited: Z. Mi, “AlGaN nanowire deep ultraviolet opotelectronics,” 33rd North American Conference on Molecular Beam Epitaxy, Galveston Island, TX, Oct. 15-18, 2017.
D. A. Laleyan1, S. Zhao, Y. Wang, E. T. Reid, K. Mengle, E. Kioupakis, and Z. Mi, “Effect of Growth Temperature on the Structural and Optical Properties of Few Layer Hexagonal Boron Nitride by Molecular Beam Epitaxy,” 60th Electronic Materials Conference, Santa Barbara, CA, June 27-29, 2018.
S. Zhao, S. Sadaf, X. Liu, and Z. Mi, “AlGaN Nanowire Tunnel Junction Light Emitting Diodes and Lasers,” International Symposium on Semiconductor Light Emitting Devices, Banff, Canada, Oct. 8-12, 2017.
S. M. Sadaf, S. Zhao, Y.-H. Ra, I. Shih, and Z. Mi, “Molecular Beam Epitaxial Growth and Characterization of n-GaN/Al/p-AlGaN Tunnel Junction Nanowire Heterostructure,” International Symposium on Semiconductor Light Emitting Devices, Banff, Canada, Oct. 8-12, 2017.
X. Liu, S. Zhao, B. H. Le, and Z. Mi, “Deep ultraviolet AlGaN Nanowire Light Emitting Diodes by Selective Area Epitaxial Growth,” International Symposium on Semiconductor Light Emitting Devices, Banff, Canada, Oct. 8-12, 2017.
D. A. Laleyan, S. Zhao, S. Y. Woo, H. N. Tran, H. B. Le, T. Szkopek, H. Guo, G. A. Botton and Z. Mi, “AlN/h-BN Nanowire Heterostructures for Deep Ultraviolet Photonics,” International Symposium on Semiconductor Light Emitting Devices, Banff, Canada, Oct. 8-12, 2017.
Invited: Zetian Mi, Xianhe Liu, and Kishwar Mashooq, “AlGaN Surface Emitting Ultraviolet Laser Diodes,” International Workshop on Ultraviolet Materials and Devices, Kunming, China, Dec. 9-12, 2018.
Invited: Z. Mi, P. Wang, D. Laleyan, X. Liu, and Y. Wu, Ultrahigh Temperature MBE Growth of h-BN and AlN for Ultraviolet Photonic and Excitonic Devices, IEEE Research and Applications of Photonics in Defense (RAPID) Conference Miramar Beach, Aug. 19-21, 2019.
Invited: X. Liu, D. Laleyan, P. Wang, and Z. Mi, AlGaN and BN Nanocrystals: Path Towards High Efficiency Deep Ultraviolet LEDs and Surface Emitting Laser Diodes, SPIE Optics and Photonics, San Diego, CA, Aug. 11-15, 2019.
Invited: Z. Mi, X. Liu, Y. Sun, and D. Laleyan, III-Nitride Nanocrystal Laser Diodes and Integrated Photonics, OSA Advanced Photonics Congress, July 29 - Aug. 1, 2019.
Plenary: Z. Mi, “Emerging applications of III-nitride nanocrystals,” International Conference on Nitride Semiconductors, July 7-12, 2019, Bellevue, Washington.

Honors and Awards: PhD student David Laleyan received Best Student Paper Award for his paper “AlN/h-BN Nanowire Heterostructures for Deep Ultraviolet Photonics” from the 11th International Symposium on Semiconductor Light Emitting Devices.

PhD student Xianhe Liu received Best Student Paper Award for his paper “Deep ultraviolet AlGaN Nanowire Light Emitting Diodes by Selective Area Epitaxial Growth” from the 11th International Symposium on Semiconductor Light Emitting Devices.

Zetian Mi has been elected Fellow of SPIE and Fellow of OSA.

Zetian Mi recognized as a most highly prolific author in Nano Letters.

Zetian Mi received IEEE Photonics Society Distinguished Lecturer Award

Zetian Mi received David E. Liddle Research Excellence Award, University of Michigan

Protocol Activity Status:

Technology Transfer: Some IP related to this work was licensed to NS Nanotech, Inc., which was co-founded by Z. Mi. The University of Michigan and Mi have a financial interest in the company.

PARTICIPANTS:

Participant Type: Graduate Student (research assistant)

Participant: Hee Woo Kim
Person Months Worked: 2.00 **Funding Support:**
Project Contribution:
National Academy Member: N

Participant Type: Graduate Student (research assistant)
Participant: David Laleyan
Person Months Worked: 6.00 **Funding Support:**
Project Contribution:
National Academy Member: N

Participant Type: Graduate Student (research assistant)
Participant: Xianhe Liu
Person Months Worked: 1.00 **Funding Support:**
Project Contribution:
National Academy Member: N

Participant Type: Graduate Student (research assistant)
Participant: Xiwen Liu
Person Months Worked: 1.00 **Funding Support:**
Project Contribution:
National Academy Member: N

Participant Type: Graduate Student (research assistant)
Participant: Kishwar Mashooq
Person Months Worked: 2.00 **Funding Support:**
Project Contribution:
National Academy Member: N

Participant Type: Graduate Student (research assistant)
Participant: Ayush Pandey
Person Months Worked: 3.00 **Funding Support:**
Project Contribution:
National Academy Member: N

Participant Type: Graduate Student (research assistant)
Participant: Yuanpeng Wu
Person Months Worked: 5.00 **Funding Support:**
Project Contribution:
National Academy Member: N

Participant Type: Postdoctoral (scholar, fellow or other postdoctoral position)
Participant: Yi Sun
Person Months Worked: 2.00 **Funding Support:**

RPPR Final Report
as of 06-Sep-2022

Project Contribution:
National Academy Member: N

Participant Type: PD/PI
Participant: Zetian Mi
Person Months Worked: 2.00 **Funding Support:**
Project Contribution:
National Academy Member: N

International Travel:

CAN	5 days
JPN	10 days
DEU	5 days
FRA	5 days
SGP	2 days
SWE	2 days
CHN	5 days

International Collaboration:

CAN

Partners

,

I certify that the information in the report is complete and accurate:
Signature: Zetian Mi
Signature Date: 9/5/22 12:32PM

Project Report

1. Statement of the Problem Studied

Mid and deep ultraviolet (UV) light sources, including light emitting diodes (LEDs) and laser are required for many demanding applications ranging from materials processing, surface treatment, chemical and biological analysis to water purification and disinfection. To date, there have been no commercial laser diodes with emission wavelengths shorter than 370 nm [1]. The poor performance of UV optoelectronic devices is directly related to the presence of large densities of dislocations (typically in the range of 10^8 cm^{-2}, or higher), strong polarization field and the related quantum-confined Stark effect, and extremely poor *p*-type conductivity of AlN and AlGaN (hole concentration in AlN typically limited to ~ 10^{13} cm^{-3}, or less) [2-7].

In this context, significant progress has been made in the epitaxy and characterization of AlGaN nanoscale heterostructures [8-11]. Nearly dislocation-free AlGaN nanowires, or nanowalls can be grown directly on low-cost, large-area Si and sapphire substrate [10-14]. We have discovered, both experimentally and theoretically, that Mg-dopant incorporation is significantly enhanced in nearly defect-free nanoscale III-nitride structures compared to their bulk counterparts [10, 15-17], thereby leading to very efficient *p*-type conduction in wide bandgap Al-rich AlGaN that was not previously possible [18]. In this project, we propose to investigate the design, epitaxy, fabrication and testing of AlGaN nanowire and nanowall laser diodes. The device heterostructure consists of AlGaN nanostructures grown on sapphire or Si substrate using the technique of selective area growth by molecular beam epitaxy. Some of the major achievements of this project include: i) Achievement of selective area epitaxy of AlGaN nanowires across nearly the entire compositional range; ii) First demonstration of electrically pumped AlGaN nanowire photonic crystal UV laser diode, which operates at 369.5 nm at room temperature with a low threshold current density of 10.6 mA under continuous wave operation; iii) Demonstration of electrically injected plasmonic UV quantum dot laser diodes, which are the shortest wavelengths ever reported for any semiconductor plasmonic lasers. These studies provide a viable path for the achievement of low threshold mid and deep UV laser diodes.

2. Summary of the Most Important Results

2.1. Epitaxial Growth and Characterization of Al-rich AlGaN Nanostructures for High Efficiency UV Laser Diodes

a) <u>AlGaN Nanowire Arrays across Nearly the Entire Compositional Range</u>

The previously reported AlGaN nanowires have been largely formed spontaneously, with random variations in size, spacing, and geometry. Such issues are addressed by using the technique of selective area epitaxy. Prior tour work, there had been no demonstration of AlGaN nanowires emitting in the UV-C band by selective area epitaxy. Shown in Figure 1(a) is a scanning electron microscope (SEM) image of GaN/$Al_xGa_{1-x}N$ nanowire arrays, which exhibit controlled size and spacing and well-defined hexagonal morphology, with a very high degree of uniformity. Detailed scanning transmission electron microscopy studies further confirm that an

Al-rich AlGaN shell structure is spontaneously formed surrounding the nanowires, which can suppress nonradiative surface recombination. Photoluminescence (PL) spectra of these AlxGa1-xN nanowire arrays were measured at room-temperature. Illustrated in Figure 1(b), strong PL emission from 210 nm to 327 nm was measured from $Al_xGa_{1-x}N$ nanowires grown with different Al compositions. The correlation between the energy bandgap of $Al_xGa_{1-x}N$ and Al composition x can be approximately derived from Eqn. (1) below.

$$E_g = 6.015x + 3.39(1-x) - 0.98x(1-x) \quad (1)$$

For comparison, previous studies on selective area epitaxy of $Al_xGa_{1-x}N$ nanowires were largely limited to Al composition below 40%. The realization of high quality Al-rich $Al_xGa_{1-x}N$ nanowire arrays by selective area epitaxy provides a distinct opportunity to demonstrate high efficiency nanowire photonic crystal light emitters including LEDs and laser diodes operating in UV-C band, to be described next.

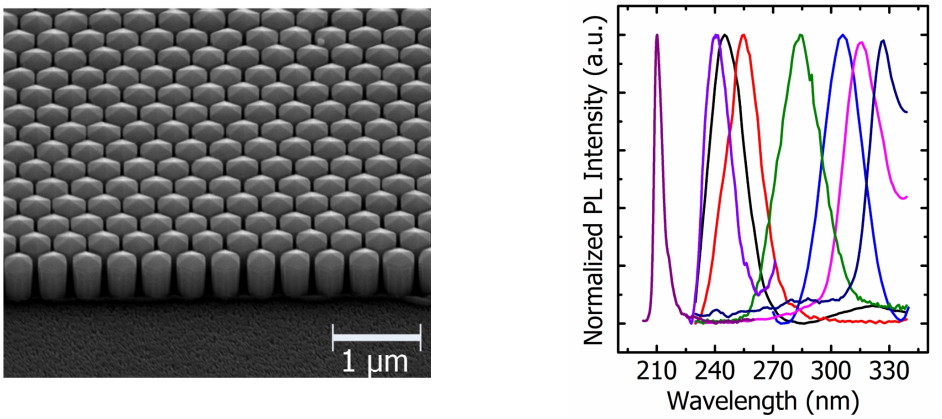

Figure 1. (a) An SEM image of GaN/AlxGa1-xN nanowire arrays grown by selective area epitaxy. (b) Normalized room-temperature photoluminescence (PL) spectra of $Al_xGa_{1-x}N$ nanowire arrays with Al compositions tuned from ~20% to 100%.

b) Epitaxy and Characteristics of p-Type AlN Nanostructures and LEDs

To achieve high performance laser diodes, it is imperative to have efficient hole transport and injection in AlGaN. Prior to our work, however, free hole concentrations of AlN can only be measured at ~10^{10} cm^{-3} level at room temperature for epilayer structures, which is more than *seven* orders of magnitude lower than what is commonly required (~10^{17}–10^{19} cm^{-3}) for practical optoelectronic devices. Magnesium (Mg), the common *p*-type dopant of III-nitrides, has a prohibitively large activation energy E_A for AlN, which results in negligible doping efficiency at room temperature. Moreover, during the epitaxy of Mg-doped AlN, the Fermi level is shifted towards the valence band edge, significantly reducing the formation energy for nitrogen-vacancy as well as donor-like point defect and impurity incorporation. We found that such fundamental material issues of AlN can be addressed through nonequilibrium epitaxy of nanostructures. During the epitaxy of N-polar AlN nanostructures, N-rich conditions are commonly used. The formation energy of N-vacancy related defects can be increased by nearly 3 eV under N-rich epitaxy condition, compared to conventional N-poor condition, thereby suppressing N-vacancy related defect formation. Moreover, the formation energy for Al-substitutional Mg-dopant

incorporation is drastically reduced by ~2 eV under N-rich epitaxy, which can significantly enhance Mg-dopant incorporation.

Previously reported planar *c*-plane AlN LEDs had a turn-on voltage ~30 V. With optimized growth conditions, we have investigated the electrical characteristics of AlN nanowire LEDs. Figure 2a shows typical room-temperature current-voltage (*I-V)* characteristics of as-fabricated AlN nanowire LEDs, which has a small reverse leakage current ~10 nA at -5 V and strong electroluminescence emission at ~210 nm. Under forward bias, the electrical characteristics exhibit three different trends. Region I is characterized by the presence of a carrier-injection barrier $\emptyset_{b1}$ of 2.2 eV related to the large conduction band offset between GaN and AlN. In Region II, the obtained minimum ideality factor is 4.6 at 2.4 V, but increases drastically with increasing voltage. In Region III, the device shows a turn-on voltage ~5 V, which is significantly smaller compared with previously reported planar AlN diodes and is largely determined by the energy bandgap of AlN. With further increasing voltage, injection current is limited by ohmic potential drop across the diodes. We measured the *I-V* characteristics of AlN LEDs with different Mg doping concentrations. The obtained minimum ideality factor shows a decreasing trend from 14.9 to 3.6 with increasing Mg doping concentrations from approximately 1×10^{19} to 6×10^{19} cm^{-3}. This observation rules out the possibility that the large ideality factors of AlN LEDs are the results of sum of the ideality factors of several rectifying junctions as proposed by Shah *et al*.

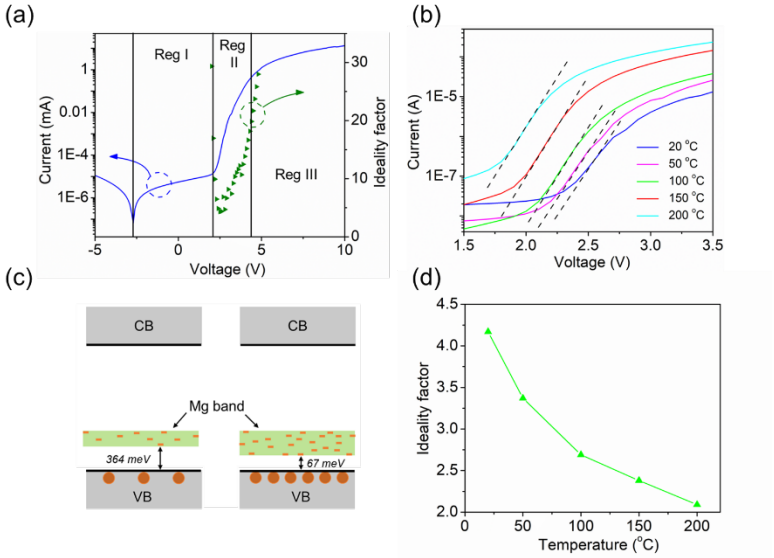

Figure 2. a) *I-V* characteristics of AlN nanowire LEDs measured at room temperature, wherein three regions with different slopes can be identified. b) Temperature-dependent *I-V* characteristics of AlN nanowire LEDs measured in the temperature range of 20-200 ºC. c) Illustration of the Mg acceptor energy levels under relatively low (left) and high (right) doping concentrations. The dispersion of Mg acceptor energy levels under very high concentrations can lead to significantly reduced activation energy (right). d) Variations of the minimum ideality factors vs. measurement temperature.

We further performed temperature-dependent *I-V* measurements. Illustrated in Figure 2b, the measured currents between 2.5 and 3.5 V show a monotonic increasing trend with increasing temperature. The dashed black lines in Figure 3b indicate the slopes of forward *I-V*, which are

largely invariant from room temperature to 200 °C. The ideality factor, derived by $n = \frac{kT}{q}\left[\frac{dV}{d(lnI)}\right]$, therefore shows a strong temperature dependence. Previous reports attributed temperature-independent slopes of (log*I*)-vs.-*V* plots to the involvement of charge carrier tunneling. The total forward current *J* of the *p-i-n* diode can be expressed as the sum of diffusion component J_D in the neutral region (both *p* and *n* layers) and the tunneling current J_T in the depletion region,

$$J = J_{D0}\left[\exp\left(\frac{qV_A}{kT}\right) - 1\right] + J_{T0}\left[\exp\left(\frac{qV_A}{E_T}\right) - 1\right] \quad (1)$$

where V_A is the voltage applied through the AlN *p-i-n* diode, and E_T is the characteristic tunneling energy. Here other factors such as radiative and nonradiative carrier recombination that could lead to larger ideality factors are not considered. Using Eqn. (1), E_T of 364 meV is obtained for the AlN LED with a Mg concentration of ~1×10^{19} cm^{-3}. E_T values on this order have been attributed to deep-level-assisted electron (hole) tunneling,[38] such as the deep Mg acceptor levels in AlN, which are in the range of 500-600 meV. In this study, it is observed that E_T decreases to 67 meV for the AlN LED with a Mg concentration of ~6×10^{19} cm^{-3}. Very high Mg impurity concentrations in AlN can result in the formation of an impurity band, schematically shown in Figure 2c, instead of localized impurity levels, due to impurity-impurity interactions.[22, 40, 41] With increasing Mg concentration, the dispersion of Mg acceptor energy levels can lead to reduced ionization energy for a portion of Mg dopants, illustrated in the right panel of Figure 2c. This is consistent with the observation of a reduction of the characteristic tunneling energy from 364 meV to 67 meV with increasing Mg concentrations from ~1×10^{19} cm^{-3} to 6×10^{19} cm^{-3}. At elevated temperatures, hole concentrations in the impurity band is increased, and diffusion current becomes more dominant, which leads to a reduction of the ideality factor, shown in Figure 2d. The derived E_T value of 67 meV suggests that the ionization energy of Mg dopants can be effectively reduced by nearly one order of magnitude for AlN nanostructures grown under N-rich epitaxy conditions, compared to that of conventional planar AlN, thereby leading to AlN LEDs with excellent electrical performance. This study may also offer a path to address the poor current conduction of other ultra-wide bandgap semiconductors.

c) Development of AlGaN nanowall heterostructures for low threshold, high power laser diodes

In parallel, we have studied the epitaxial growth and characterization of Al(Ga)N nanowall structures, which are well suited to realize low threshold, high power edge emitting laser diodes. We have demonstrated, for the first time, an AlN nanowall LED, which can operate efficiently at ~210 nm. The devices exhibit excellent current-voltage characteristics, including a turn-on voltage of 7 V and current densities > 170 A/cm^2 at 12 V. In this study, GaN nanowall structures were first created on n-type GaN template on sapphire substrate using e-beam lithography and dry etching techniques. The wall widths were varied in the range of 100 nm to 1 μm. Shown in Fig. 3, it is seen that AlN nanowalls exhibit smooth surface morphology on both the top and lateral surfaces, due to the efficient surface stress relaxation. Optical properties of AlN nanowall structures were studied using temperature and power-dependent photoluminescence measurements. Shown in the inset Fig. 4(a) is the PL spectrum of AlN nanowalls with wall widths ~410 nm. A distinct emission peak at ~210 nm from free exciton emission was measured at room-temperature. In addition, two phonon replicas, with energy separation ~100 and 200 meV from the free exciton emission, respectively, were also clearly measured, which are indicated by the arrows shown in the inset of Fig. 4(a). The direct measurements of phonon

sideband emission at room-temperature suggests superior material quality of the presented AlN nanowalls.

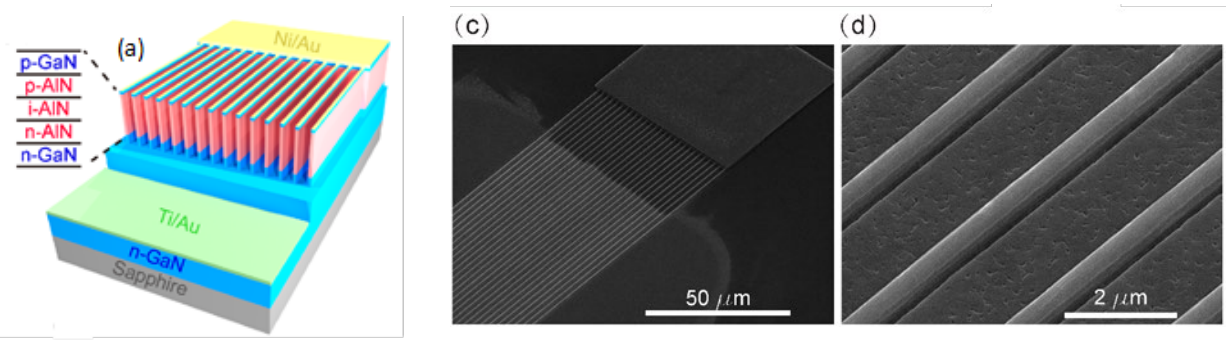

Figure 3. (a) Schematic of an AlN nanowall LED grown on GaN template on sapphire substrate. The device heterostructure is shown in the inset. (b) and (c) SEM images of AlN nanowall structures.

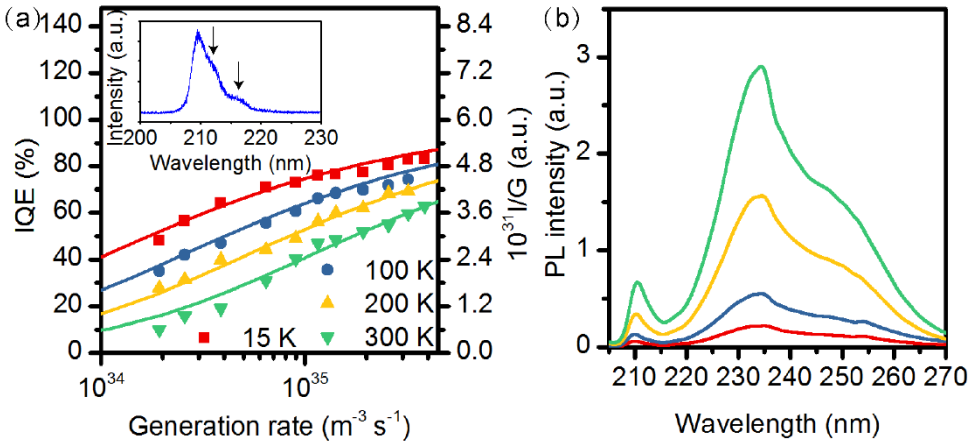

Figure 4. (a) Plot of the internal quantum efficiency (IQE) (left axis) and relative external quantum efficiency (right axis) of an AlN nanowall structure vs. carrier generation rate measured at different temperatures. PL spectrum of the AlN nanowall structure measured at room-temperature is shown in the inset. The arrows indicate phonon sideband emissions. (b) PL spectra of Mg-doped AlN nanowall structures measured under excitation powers varying from 50 mW to 300 mW at room-temperature.

The IQE was calculated by studying the PL spectra of the non-doped AlN nanowall samples at different temperatures and under different excitation powers using the following rate equations.

$$G = AN + BN^2 + CN^3 \quad (2)$$

$$I = \theta BN^2 \quad (3)$$

$$\eta_i = I / (\theta G) \quad (4)$$

where G is the carrier generation rate, A is the Shockley–Read–Hall recombination coefficient, B is the radiative recombination coefficient, C is the Auger recombination coefficient, N is the

carrier concentration, I is the measured PL intensity, and η_i is the IQE. θ is a constant and is determined by the optical setup. in Fig. 4(a) is the calculated IQE vs. carrier generation rate and the measured relative external quantum efficiency ($\mathrm{EQE} \propto I / G$). The simulation agrees well with the experimental results in the wide temperature range of 15 K to 300 K and for various carrier generation rates. It is seen that the IQE exhibited an increasing trend with increasing excitation and decreasing temperature. At room temperature, it can reach up to 60%, suggesting superior material quality. Strong photoluminescence emission at room-temperature was also measured for Mg-doped AlN nanowall structures. Shown in Fig. 4(b) are the PL spectra for nanowall arrays with 410 nm widths under varying excitation powers. Besides the free exciton emission peak at ~210 nm, there is another peak at 234 nm due to Mg-acceptor related transition. The shoulder at ~250 nm of the emission spectra is attributed to transitions of electrons bound to nitrogen vacancy with triple positive charges (V_N^{3+}) and Mg acceptors.

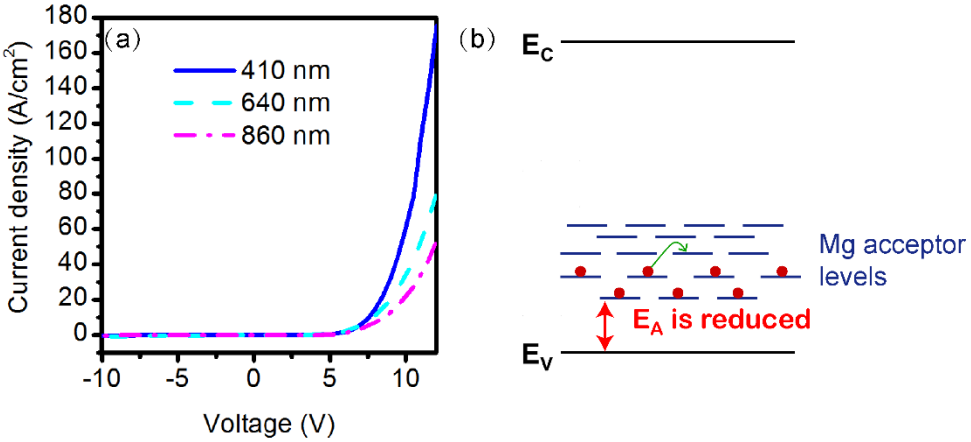

Figure 5. (a) Current-voltage characteristics of AlN nanowall LEDs with different wall widths measured at room-temperature. (b) Schematic illustration of the formation of an Mg impurity band and the reduced activation energy for a portion of the Mg acceptors, due to the significantly broadened Mg acceptor level distribution.

We have subsequently investigated the fabrication and characteristics of AlN nanowall LEDs. Shown in Fig. 5(a) are the current-voltage characteristics of AlN nanowall LEDs with wall widths of 410 nm, 640 nm, and 860 nm, respectively. The length of each nanowall structure in these LED devices is 120 μm. The devices exhibit excellent current-voltage characteristics, with turn-on voltages ~7 V, which is significantly smaller than that of previously reported c-plane AlN epilayer LEDs. The large concentrations of Mg dopants leads to the formation of Mg impurity band in AlN nanowalls as well as significantly broadened acceptor level distributions, evidenced by the broad PL spectral linewidth associated with Mg acceptor transition shown in Fig. 4(b). Consequently, a portion of Mg acceptors have significantly reduced activation energy, schematically shown in Fig. 5(b), thereby enabling efficient hole conduction in AlN that was previously difficult to achieve in AlN epilayers. AlN nanowall LEDs exhibit strong electroluminescence (EL) emission.

In summary, we have demonstrated AlN nanowall LEDs that can exhibit significantly improved optical and electrical performance, compared to conventional AlN epilayer devices. Detailed

temperature and power-dependent photoluminescence measurements and rate equation analysis suggested that the AlN nanowalls exhibited relatively high internal quantum efficiency (~60%) at room-temperature. Such AlN nanowall devices are well suited for large area, high power applications. It is envisioned that Al(Ga)N nanowall heterostructures will emerge as a viable architecture for achieving high efficiency deep UV LEDs, laser diodes, and photodetectors.

2.2. Electrically Injected AlGaN Nanowire Photonic Crystal Ultraviolet Laser

Recent theoretical studies have suggested that defect-free nanowire photonic crystal structures can behave as mirrorless resonant cavities with high quality factor and fineness. Prior to our work, however, there have been no reports on such photonic crystal lasers operating in the UV wavelength range. In this context, we have studied the design, fabrication, and characterization of defect-free AlGaN nanowire photonic crystal lasers. Using the finite-element method, we have studied the simulation of defect-free AlGaN nanowire photonic crystal structures as a topological high-Q resonator. The simulation is performed using the RF module of Comsol Multiphysics. A topological resonator is expected to operate near the band edge of a photonic crystal structure with an arbitrary shape. In this study, a photonic crystal with band edge around 370 nm is designed as an example. The lattice constant *a* of the nanowire photonic crystal is 400 nm, and the spacing between nanowires is ~36 nm. The effective refractive index is ~2.49 for GaN/$Al_xGa_{1-x}N$ nanowires. The corresponding band structure for transverse magnetic polarization (***E*** in parallel with growth direction) is shown in Fig. 6. The normalized frequency a/λ for the operation wavelength 370 nm is ~1.08, which is found to be near the Γ point of the band shown in red color. It is therefore expected such a photonic crystal structure with an arbitrary shape to behave like a topological high Q-factor cavity near this wavelength.

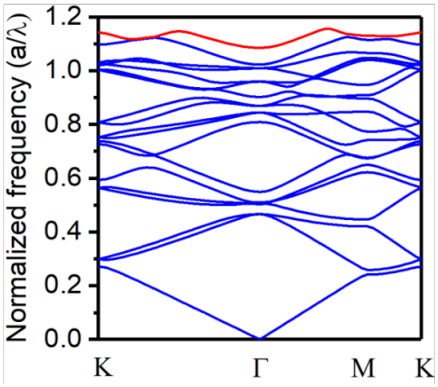

Figure 6. Band structure of the designed photonic crystal structure targeted to operate at a/λ=1.08.

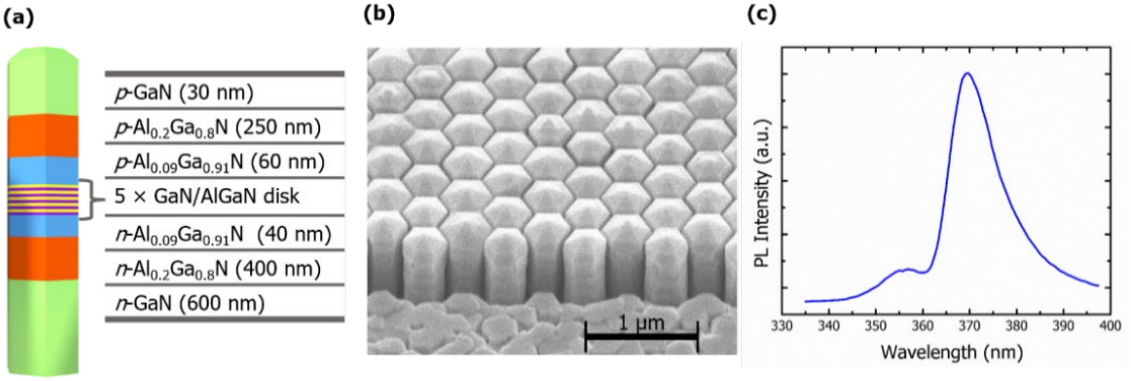

Figure 7. (a) Schematic illustration of GaN/$Al_xGa_{1-x}N$ multiple quantum disk nanowire structure. (b) Titled view SEM image of GaN/$Al_xGa_{1-x}N$ nanowire arrays grown by selective area epitaxy. (c) Room-temperature photoluminescence spectrum of GaN/$Al_xGa_{1-x}N$ nanowire arrays.

Extensive growth optimization was performed to achieve GaN/$Al_xGa_{1-x}N$ nanowire photonic crystals. Vertically aligned GaN/$Al_xGa_{1-x}N$ nanowire arrays, schematically illustrated in Fig. 7(a), were selectively grown in the opening apertures by MBE. Figure 7(b) shows a scanning electron microscope (SEM) image of the GaN/$Al_xGa_{1-x}N$ nanowire arrays taken at a tilted angle. It is seen that the nanowires exhibit a high level of size uniformity. Illustrated in Fig. 7(c), strong emission of GaN/$Al_xGa_{1-x}N$ nanowire arrays at ~370 nm can be clearly measured. The PL peak emission at ~355 nm originates from the $Al_xGa_{1-x}N$ guide layer.

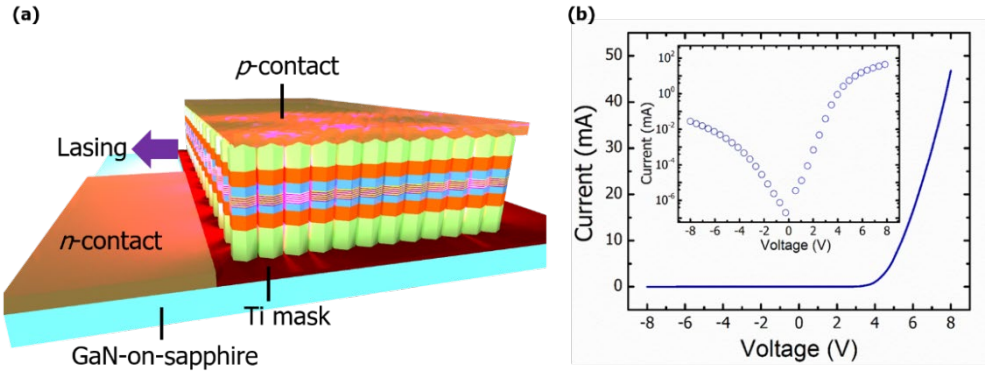

Figure 8. (a) Schematic of GaN/$Al_xGa_{1-x}N$ nanowire photonic crystal laser grown by selective area epitaxy. (b) Current-voltage characteristics of GaN/$Al_xGa_{1-x}N$ nanowire photonic crystal laser. Inset: *I-V* characteristics plotted in semi-log scale.

Subsequently, the nanowire arrays were fabricated into photonic crystal lasers using standard photolithography, e-beam lithography, dry etching and contact-metallization techniques. The operation of the GaN/$Al_xGa_{1-x}N$ nanowire photonic crystal lasers is schematically illustrated in Fig. 8(a). The current-voltage (*I-V*) characteristics of GaN/$Al_xGa_{1-x}N$ photonic crystal lasers are shown in Fig. 8(b). The fabricated nanowire photonic crystal lasers exhibit good current-voltage characteristics. The device shows a relatively low turn on voltage of ~ 4V and exhibit a very low leakage current of ~27 µA at -8V as indicated in the inset.

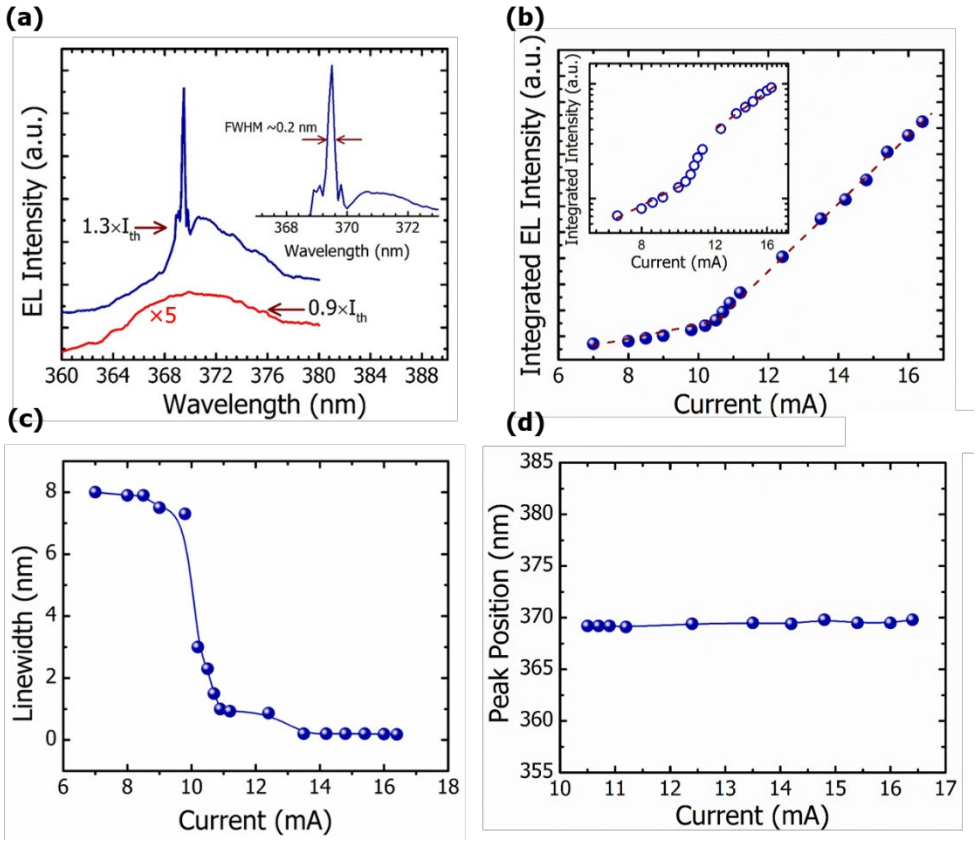

Figure 9. (a) Room-temperature electroluminescence spectra of GaN/$Al_xGa_{1-x}N$ photonic crystal lasers below (red) and above (blue) threshold current. The spectra are vertically shifted for display purpose. (b) Integrated EL intensity of lasing emission as a function of injection current. Inset: Variation of integrated EL intensity vs. current in log scale. (c) EL spectral linewidth vs. current. (d) Variation of lasing peak position vs. current.

The lasing characteristics of such devices were investigated under electrical injection under continuous-wave operation at room-temperature. Figure 9(a) shows the room-temperature EL spectra of GaN/$Al_xGa_{1-x}N$ photonic crystal lasers at injection currents below and above threshold current (I_{th}). It is observed that, with increasing injection current, a sharp peak emerged and superimposed on the broad background emission. Above threshold, the EL spectrum shows a sharp peak centered at 369.5 nm with full-width-at-half-maximum (FWHM) of ~0.2 nm. The light-current (*L-I*) characteristics of photonic crystal laser are illustrated in Fig. 9(b), clearly showing a threshold current of ~10.6 mA. The relatively low threshold current is directly related to the dislocation-free AlGaN nanowire heterostructures, the core-shell nanowire arrays with suppressed surface recombination, and the topological high-Q resonance of defect-free nanowire photonic crystals. The variations of integrated EL intensity and linewidth of the lasing peak as a function of injection current in the logarithmic scale are plotted in the inset of Fig. 9(b) and Fig. 9(c), respectively. The S-shaped *L-I* curve, together with the significant reduction of spectral linewidth near threshold confirm the evolution from spontaneous emission, amplified spontaneous emission to linear lasing emission with increasing injection current, providing

unambiguous evidence for the achievement of lasing. Shown in Fig. 9(d) are variations of the laser peak position with increasing injection current. It is observed that the peak position exhibits a negligible change as injection current increases, suggesting an extremely stable lasing operation.

In summary, we have demonstrated a low threshold electrically injected semiconductor UV laser by utilizing defect-free AlGaN nanowire photonic crystals. The photonic crystal lasers exhibit a peak emission at 369.5 nm with a very low threshold current. The spectral linewidth is as narrow as ~0.2 nm. The device performance can be further improved by optimizing the design of nanowire photonic crystal optical cavity. Such nanowire photonic crystals provide a unique approach for achieving semiconductor laser diodes in the UV-B and UV-C bands. This work also bridges the gap between conventional single nanowire devices and large-area laser diodes that are often required for practical applications.

2.3 Ultralow threshold Quantum Dot UV Laser Diodes

Small size ultraviolet (UV) lasers are important for a broad range of applications including disinfection, sensing, Raman spectroscopy, analytic chemistry, and high-resolution lithography. Success in developing such semiconductor devices, however, has been extremely challenging, due to the difficulty in confining light to very small dimensions. To date, there have been only few reports on plasmonic lasers operating in ultraviolet (UV) wavelength range, which all exhibit very a low quality-factor (Q-factor) ~100-200. This is ascribed to material dissipation, imperfect structure, and the bottleneck of achieving high quality metal layer, which limits surface plasmons coupling efficiency and the realization of low-loss optical confinement. Consequently, the operation wavelengths of plasmonic lasers have been restricted within the UV-AI band (340-400 nm) under optical pumping only. Additionally, it has remained extremely challenging to achieve electrically injected plasmonic lasers operating at any wavelengths. In this context, we have studied a new type of UV plasmonic lasers to address the above-mentioned issues. In our design, photon confinement is achieved in the plasmonic wedge mode formed on a microscale stripe coated with an ultrathin epitaxial Al layer as a metal cavity coupling with a wide bandgap aluminum-gallium-nitride (AlGaN) quantum dot layer. It is known that the Q-factor of plasmonic lasers is strongly dependent on the strength of stored energy over the dissipated energy, in other words, optical confinement, which is governed by high quality metal layer, plasmonic mode and gain media. Thus, an ultrathin Al layer, ideal candidate metal for UV plasmonics, is epitaxially deposited under ultrahigh vacuum conditions. In the unique design, self-organized AlGaN quantum dots are incorporated as the gain medium, which is positioned in proximity of the metal cavity. The utilization of AlGaN quantum dots can significantly reduce nonradiative surface recombination and therefore contributes to the very low lasing threshold. In addition, AlGaN has intrinsically large gain and exhibits extremely low surface recombination. AlGaN-based nano/micro-scale structures also exhibit superior characteristics of dislocation-free and efficient current conduction. These intriguing properties make it attractive to study plasmonic-based UV lasers to break the efficiency bottleneck of UV optoelectronics. The AlGaN UV plasmonic lasers exhibit excellent performance, including a very low threshold current of ~75 μA under continuous wave operation at room-temperature.

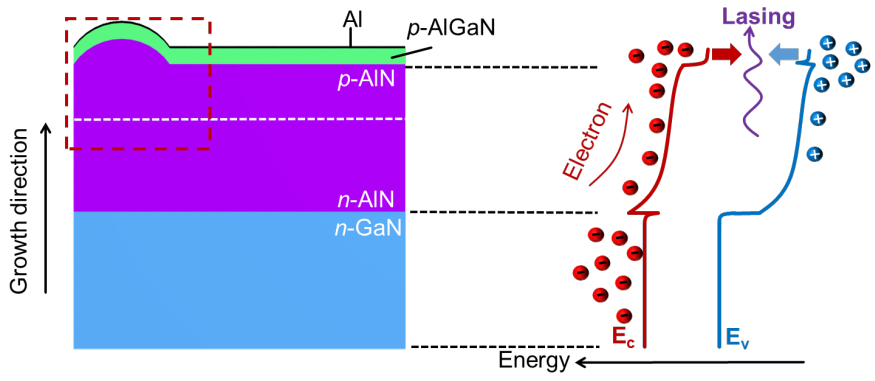

Figure 10: Structure design and operation of AlN/AlGaN quantum dot plasmonic laser. a, Schematic of the cross section near the edge of a stripe. The box indicates the simulation regions. The arrow indicates growth direction. b, Band diagram of the AlN/AlGaN structure. Dashed lines are eye-guided lines.

Schematically shown in Fig. 10a, the AlGaN plasmonic laser structure consists of an *n*-GaN buffer layer, *n*- and *p*-AlN layers and a thin *p*-AlGaN quantum dot top layer. The cross-sectional profile has a bump-like cavity on the edge of the stripe Figure 10b shows the band diagram of AlN/AlGaN structure. Under electrical injection, electrons overflow and recombine radiatively with holes in the *p*-AlGaN layer due to the much higher hole concentration than that in the *p*-AlN. The *p*-AlGaN layer have quantum-dot-like features due to the lattice mismatch with the underneath *p*-AlN layer, which can offer strong quantum confinement and minimize surface recombination.

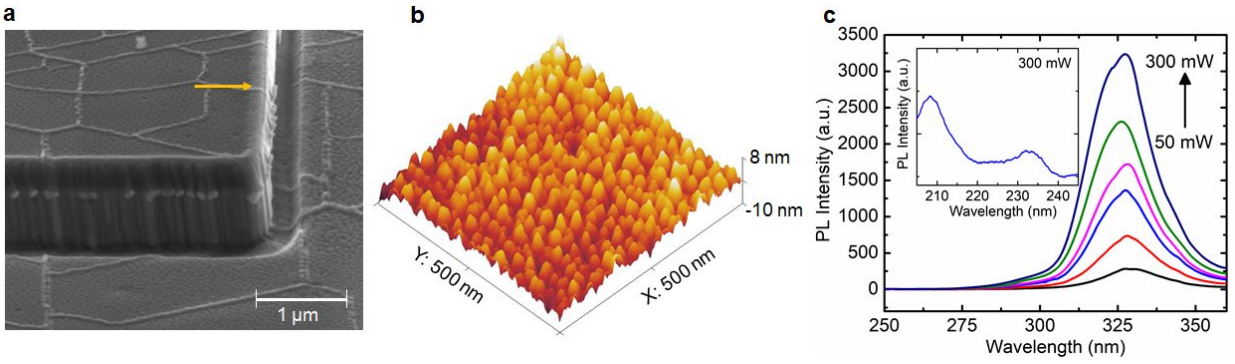

Figure 11. Characterization of AlN/AlGaN quantum dot plasmonic laser. a, A 70º-titled SEM image of AlN/AlGaN quantum dot plasmonic laser, clearly showing the bump-like cavity formed at the stripe edges indicated by the arrow. b, AFM surface topography of AlN/AlGaN plasmonic laser showing high density of quantum dots. c, Photoluminescence spectra measured at room-temperature under different excitation powers varying from 50 mW to 300 mW. Inset: Photoluminescence emission of AlN layer under excitation power of 300 mW.

Shown in Fig. 11a is an SEM image of AlN/AlGaN quantum dot plasmonic stripe lasers. Structural characterization of the AlGaN quantum dot stripe structure was carried out using atomic force microscopy (AFM), shown in Fig. 11b. The dot density is estimated to be ~2 × 10^{11} cm^{-2}. The stripe laser structure exhibits strong photoluminescence (PL) emission at room-temperature. Figure 11c shows PL spectra of AlN/AlGaN stripes under different excitation powers. Subsequently, stripe structures were fabricated into plasmonic laser devices using standard photolithography, e-beam lithography, isolation and contact-metallization techniques.

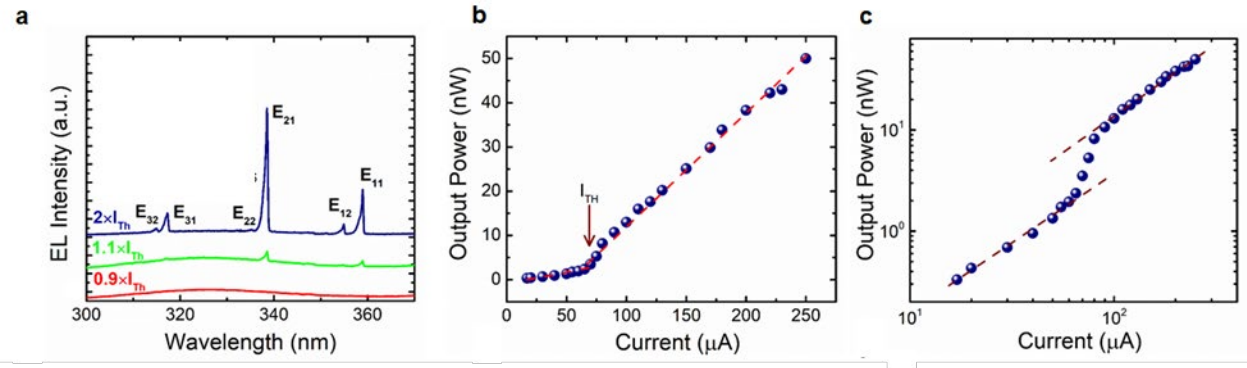

Figure 12. Characterization of AlN/AlGaN quantum dot plasmonic laser. a, Room-temperature electroluminescence spectra of AlN/AlGaN quantum dot plasmonic laser below (red) and above (green, blue) threshold current. The spectra are vertically shifted for display purpose. Inset: Magnified electroluminescence spectra. b, Output power of emission peak of lasing mode E_{21} at 338.5 nm as a function of injection current, clearly showing threshold current I_{Th} ~75 μA. c, Variations of output power in log scale at 338.5 nm with increasing injection current, respectively. The S-shaped L-I curve with increasing current further confirm lasing operation.

The lasing characteristics of such devices were investigated by electrical injection under continuous wave operation at room-temperature. Figure 12a shows the room-temperature electroluminescence (EL) spectra of AlN/AlGaN stripe devices at different injection currents below and above threshold current (I_{Th}). It is observed that, by increasing injection current, sharp peaks emerge and superimpose on the broad background emission. At an injection current above I_{Th}, EL spectrum of stripe laser diode shows a sharp peak centered at 338.5 nm. Other lasing modes are also observed. The three main lasing peaks (E_{11}, E_{21}, and E_{31}) are in good agreement with the calculations. The presence of shorter wavelength sub-modes of E_{12}, E_{22}, and E_{32} near the dominant E_{11}, E_{21}, and E_{31}, respectively, is likely related to longitudinal optical confinement. As the lasing peak at 338.5 nm (mode E_{21}) is the strongest one, its threshold and linewidth properties are first presented. The light-current (*L-I*) characteristics are illustrated in Fig. 12b, showing a clear threshold current I_{Th} of ~75 μA. The variations of output power as functions of injection current in the logarithmic scale are plotted in Fig. 12c. The S-shaped *L-I* curve suggests the evolution from spontaneous emission, amplified spontaneous emission to lasing emission with increasing current. At an injection current of ~250 μA, the FWHM of the lasing peak at 358.9

nm is as narrow as ~0.3 nm. This work provides a viable approach to achieve electrically injected semiconductor lasers operating in the mid and deep UV spectra and to break the efficiency bottleneck of UV optoelectronics.

3. Bibliography

[1] H. Yoshida, Y. Yamashita, M. Kuwabara, and H. Kan, "Demonstration of an ultraviolet 336 nm AlGaN multiple-quantum-well laser diode," *Appl. Phys. Lett.,* vol. 93, no. 24, p. 241106, 2008, doi: 10.1063/1.3050539.

[2] H. Hirayama *et al.*, "222-282 nm AlGaN and InAlGaN-based deep-UV LEDs fabricated on high-quality AlN on sapphire," *Phys. Status Solidi A,* vol. 206, no. 6, pp. 1176-1182, 2009, doi: 10.1002/pssa.200880961.

[3] Y. Taniyasu, M. Kasu, and T. Makimoto, "Increased electron mobility in n-type Si-doped AlN by reducing dislocation density," *Appl. Phys. Lett.,* vol. 89, no. 18, p. 182112, 2006, doi: 10.1063/1.2378726.

[4] M. Martens *et al.*, "Performance Characteristics of UV-C AlGaN-Based Lasers Grown on Sapphire and Bulk AlN Substrates," *IEEE Photon. Technol. Lett.,* vol. 26, p. 342, 2014.

[5] Y. Taniyasu, M. Kasu, and T. Makimoto, "An aluminium nitride light-emitting diode with a wavelength of 210 nanometres," *Nature,* vol. 441, no. 7091, pp. 325-8, May 18 2006, doi: 10.1038/nature04760.

[6] J. Renard, R. Songmuang, G. Tourbot, C. Bougerol, B. Daudin, and B. Gayral, "Evidence for quantum-confined Stark effect in GaN/AlN quantum dots in nanowires," *Phys. Rev. B,* vol. 80, p. R121305, 2009, doi: 10.1103/PhysRevB.80.121305.

[7] S. F. Chichibu *et al.*, "Origin of defect-insensitive emission probability in In-containing (Al,In,Ga)N alloy semiconductors," *Nat. Mater.,* vol. 5, no. 10, pp. 810-6, Oct 2006, doi: 10.1038/nmat1726.

[8] S. D. Carnevale, T. F. Kent, P. J. Phillips, M. J. Mills, S. Rajan, and R. C. Myers, "Polarization-Induced pn Diodes in Wide-Band-Gap Nanowires with Ultraviolet Electroluminescence," *Nano Lett.,* vol. 12, no. 2, pp. 915-20, Feb 8 2012, doi: 10.1021/nl203982p.

[9] S. D. Carnevale, J. Yang, P. J. Phillips, M. J. Mills, and R. C. Myers, "Three-Dimensional GaN/AlN Nanowire Heterostructures by Separating Nucleation and Growth Processes," *Nano Lett.,* vol. 11, no. 2, pp. 866-71, Feb 9 2011, doi: 10.1021/nl104265u.

[10] S. Zhao, H. P. T. Nguyen, M. G. Kibria, and Z. Mi, "III-Nitride nanowire optoelectronics," *Progress in Quantum Electronics,* vol. 44, pp. 14-68, 2015, doi: 10.1016/j.pquantelec.2015.11.001.

[11] S. Zhao *et al.*, "Aluminum nitride nanowire light emitting diodes: Breaking the fundamental bottleneck of deep ultraviolet light sources," *Sci. Rep.,* vol. 5, p. 8332, 2015, doi: 10.1038/srep08332.

[12] Q. Wang, H. P. T. Nguyen, K. Cui, and Z. Mi, "High efficiency ultraviolet emission from AlxGa1−xN core-shell nanowire heterostructures grown on Si (111) by molecular beam epitaxy," *Applied Physics Letters,* vol. 101, no. 4, p. 043115, 2012, doi: 10.1063/1.4738983.

[13] Q. Wang *et al.*, "Optical properties of strain-free AlN nanowires grown by molecular beam epitaxy on Si substrates," *Applied Physics Letters,* vol. 104, no. 22, p. 223107, 2014, doi: 10.1063/1.4881558.

[14] Q. Wang *et al.*, "Highly efficient, spectrally pure 340 nm ultraviolet emission from AlxGa1-xN nanowire based light emitting diodes," *Nanotechnology,* vol. 24, no. 34, p. 345201, Aug 30 2013, doi: 10.1088/0957-4484/24/34/345201.
[15] S. Zhao *et al.*, "p-Type InN Nanowires," *Nano Lett.,* vol. 13, no. 11, pp. 5509-13, 2013, doi: 10.1021/nl4030819.
[16] S. Zhao *et al.*, "Tuning the Surface Charge Properties of Epitaxial InN Nanowires," (in English), *Nano Lett.,* vol. 12, no. 6, pp. 2877-2882, Jun 2012.
[17] Z. Fang *et al.*, "Si Donor Incorporation in GaN Nanowires," *Nano Lett.,* vol. 15, no. 10, pp. 6794-801, Oct 14 2015, doi: 10.1021/acs.nanolett.5b02634.
[18] A. T. Connie *et al.*, "Optical and electrical properties of Mg-doped AlN nanowires grown by molecular beam epitaxy," *Applied Physics Letters,* vol. 106, no. 21, p. 213105, 2015, doi: 10.1063/1.4921626.